

Monte Carlo investigation of drift and diffusion in semiconductor superlattices in the Wannier-Stark regime

Marcello Rosini*

Dipartimento di Ingegneria dell'Innovazione, Università di Lecce via Arnesano, Edificio Stecca, 73100 Lecce, Italy

Lino Reggiani

Dipartimento di Ingegneria dell'Innovazione, Università di Lecce and CNR-INFM National Nanotechnology Laboratory, via Arnesano, Edificio Stecca, 73100 Lecce, Italy

(Received 27 June 2005; revised manuscript received 3 August 2005; published 3 November 2005)

Hopping transport in a model superlattice Si/SiO₂ at 300 K is investigated in the Wannier-Stark approach by means of a Monte Carlo simulation. The drift velocity and longitudinal diffusion coefficient are calculated at increasing electric fields starting from conditions of negative differential mobility (NDM). We find that the Einstein relation between the mobility and the diffusion coefficient, at the given field, is fulfilled even under NDM, while, at the highest fields, the Einstein relation no longer applies and a more accurate description of the diffusion coefficient is required, owing to the presence of a complex set of hopping transitions. We found it possible to identify the crossover between the Einstein and the non-Einstein behavior in terms of an intrinsic effective length of the system which can never become smaller than the period of the superlattice. It has also been observed that the crossover corresponds to an increase of the carrier mean energy. The different diffusion regimes can be explained in terms of the carrier noise temperature.

DOI: [10.1103/PhysRevB.72.195304](https://doi.org/10.1103/PhysRevB.72.195304)

PACS number(s): 73.63.-b, 05.40.Ca, 02.70.Uu, 68.65.Cd

I. INTRODUCTION

In recent years, superlattices (SLs) have received relevant scientific and technological interest, owing to their nonlinear electrical and optical properties. In particular, at increasing electric field strength SLs exhibit a non-Ohmic behavior with the presence of a negative differential mobility (NDM) region.^{1,2} In the non-Ohmic regime, charge transport can be described in terms of hopping between Wannier-Stark (WS) states,³⁻⁵ thus SLs are good systems for studying hopping transport in semiconductor structures. In particular, there is still a lack of knowledge about drift and diffusivity properties of such systems, and to this purpose different diffusion models have been proposed in the literature.⁶⁻¹⁰ Moreover, the experimental estimation of the drift velocity and the diffusion coefficient in quantum wells and superlattices is still a difficult task.^{1,7,11,12}

In a wider context, the knowledge of drift and diffusion under high field transport is known to be a crucial issue to characterize semiconductor materials and devices.^{13,14} Also for the purposes of a microscopic physical modeling, the dependence upon the electric field of the drift and diffusion is of main importance as input parameters of device simulators. As a general trend, in bulk semiconductor materials both drift and diffusion degrade at increasing field strength by exhibiting a tendency to saturation (for the drift velocity) and a tendency to a decrease from its thermal equilibrium value (for the diffusion coefficient). A typical value of saturation drift velocity is of 10⁵ m/s and reduction of diffusivity is to one-tenth of its equilibrium value. Furthermore, because of the experimental difficulties in obtaining the field dependence of the diffusion coefficient, the possibility to use some generalized Einstein relation has proven to be of valuable help.¹⁴⁻¹⁷ To this purpose, the noise conductivity technique

has proven to be of relevant use to determine the diffusion degradation at increasing field strengths.¹⁶⁻²⁰ Recently, Arora²¹ discussed an Einstein relation, in bulks, that is different from that at zero-electric field by considering both direct and differential mobility models. In Ref. 22, the intervalley transfer of electrons is found to give results, for NDM, in agreement with Monte Carlo calculations. However, this last model uses standard scattering parameters and it is indicative of the fact that the saturation velocity, comparable to the thermal or Fermi velocity, is independent of low-field scattering parameters. Reference 7 considered Einstein relation in quantum wells and quantum wires, also providing a suggestion about useful experimental techniques.

The aim of this paper is to present a theoretical investigation of high field electronic transport in a SL in the framework of a WS approach making use of an ensemble Monte Carlo simulator of independent carriers. In this case, the low-frequency spectral density of velocity fluctuations $S_v(0)$ is related to the diffusion coefficient by the relation $S_v(0) = 4D$. Thus, the present study also addresses the problem of electron noise in analogy with previous investigations carried out in bulk materials.^{18,19}

Under thermal equilibrium, the diffusion coefficient obeys the Einstein relation $D = (2/3e)\mu\langle\epsilon\rangle$, where e is the electron charge, μ the carrier mobility, and $\langle\epsilon\rangle$ their mean kinetic energy, which for thermal electrons is given by $\langle\epsilon\rangle = \frac{3}{2}k_B T$, with k_B the Boltzmann constant and T the lattice temperature. Far from thermal equilibrium conditions, the Einstein relation is in general no longer valid and in the case of WS-hopping transport also the dependence upon the electric field of the diffusion coefficient is largely an unsolved problem.^{9,10} In this work, we will investigate to which extent the diffusion coefficient in a SL compares with a generalized Einstein relation and existing WS-hopping models.^{6,8,9}

The content of the paper is organized as follows. In Sec. II, we define the physical system under investigation and briefly describe the Monte Carlo simulator used for calculations. In Sec. III, the main results concerning the drift velocity and the diffusion coefficient are presented, and compared with analytic models. Major conclusions are then drawn in Sec. IV.

II. THE PHYSICAL MODEL

The structure of interest is a model Si/SiO₂ SL with period $L=3.1$ nm, where Si is grown along the (100) crystallographic direction.²³ The superlattice is described by the following Hamiltonian:

$$H_{\text{SL}} = H_{\text{cr}} + W_{\text{SL}} - eEz + H_{e-p}, \quad (1)$$

where H_{cr} indicates the crystal potential and kinetic energy, W_{SL} the SL potential, H_{e-p} the electron-phonon interaction, and E the applied electric field.

The interaction with phonons is treated separately using time-dependent perturbation theory and will be developed in the following, while the electric field is included in the eigenvalue problem.

Accordingly, we make use of the envelope-function and effective-mass approximations³⁷ to the unperturbed Hamiltonian so that the electronic problem is reduced to the following Schrödinger equation for the envelope function:

$$\left[-\frac{\hbar^2}{2} \nabla_i \left(\frac{1}{m(z)} \right)_{ij} \nabla_j + W_{\text{SL}}(z) - eEz \right] \mathcal{F}(\mathbf{r}) = \epsilon \mathcal{F}(\mathbf{r}), \quad (2)$$

where $[1/m(z)]_{ij}$ is the effective inverse mass tensor, $\mathcal{F}(\mathbf{r})$ is the envelope function, and $W_{\text{SL}}(z)$ is the Kronig-Penney potential, which describes the SL along the z direction. The solution of the problem is found to be²⁴

$$\mathcal{F}_{n\mathbf{k}_{\parallel}}^{\nu}(\mathbf{r}) = c e^{ik_x x} e^{ik_y y} \Phi_n(z - \nu L), \quad (3)$$

$$E_n^{\nu}(\mathbf{k}_{\parallel}) = -\nu eEL + \bar{\epsilon}_n + \frac{\hbar^2}{2m_x} k_x^2 + \frac{\hbar^2}{2m_y} k_y^2, \quad (4)$$

where ν is the spatial index of the well, n is the level index, $\bar{\epsilon}_n$ is the energy offset relative to the n th level, and $\Phi_n(z - \nu L) = \Phi_n^{\nu}(z)$ is the Wannier-Stark eigenfunction for the n th level and centered in the ν th well. For this work, we use the WS function and the energy offset obtained from the Kane representation.²⁵

The model considers only optical phonons, in particular the Si deformation potential optical mode and the SiO₂ polar and deformation potential optical modes.³¹ Moreover, we have used the scheme of confined optical phonons:³² in layered systems, the frequencies of the optical phonons²³ of the two materials do not match in general, so it is justified to assume that the optical phonon of one layer does not propagate into the other one. This is consistent with the Einstein picture for the optical phonons stating that, since the group velocity of an optical phonon excitation is negligible, the excitation does not propagate.

Hopping mechanisms are introduced through the Fermi golden rule, thus obtaining the following probability per unit

TABLE I. Values of the physical parameters used in the simulations.

Physical quantity	Value/[Ref.]
Longitudinal effective mass in Si	$m_L^* = 0.97$ [26]
Transverse effective mass in Si	$m_T^* = 0.19$ [26]
Effective mass in SiO ₂	$m^* = 0.3$ [27 and 28]
Conduction-band offset	CBO = 3.1 eV [29]
Lattice temperature	$T = 300$ K
Si optical phonon energy	$E = 60$ meV [30]
Si optical coupling constant	$D_i K = 8 \times 10^8$ eV/cm [30]
Si density	$\rho_{\text{Si}} = 2.329$ g/cm ³
Oxide nonpolar phonon energy	$E = 132$ meV [31]
Oxide optical coupling constant	$D_i K = 2 \times 10^9$ eV/cm [31]
Oxide density	$\rho_{\text{ox}} = 2.29$ g/cm ³
Oxide first polar phonon energy	$E = 63$ meV [31]
First polar optical constant	$(1/\epsilon_+) - (1/\epsilon_-) = 0.063$ [31]
Oxide second polar phonon energy	$E = 153$ meV [31]
Second polar optical constant	$(1/\epsilon_+) - (1/\epsilon_-) = 0.143$ [31]
Oxide mean polar phonon energy	$E = 108$ meV
Mean polar optical constant	$(1/\epsilon_+) - (1/\epsilon_-) = 0.2$
Electron density	$\rho_{\text{el}} = 10^{16}$ cm ⁻³

time for the transition from a state $(\nu n \mathbf{k}_{\parallel})$ to a state $(\nu' n')$ with any \mathbf{k}_{\parallel}' :

$$P(\nu' n', \nu n \mathbf{k}_{\parallel}) = \frac{\sqrt{m_x m_y}}{(2\pi)^5 \hbar^3} \left[\begin{array}{c} n_q \\ n_q + 1 \end{array} \right] \int d\theta \int dq_z c^2(\mathbf{q}) \times |\Phi_{n'}^{\nu'}(z) e^{\mp i q_z z} \Phi_n^{\nu}(z)|^2, \quad (5)$$

with¹⁴

$$c^2(\mathbf{q}) = \frac{\hbar (D_i K)^2}{2\rho V \omega_{\text{op}}} \quad (6)$$

for deformation potential optical phonons, while for polar optical phonons

$$c^2(\mathbf{q}) = \frac{e^2 \hbar \omega_{\text{op}} \mathbf{q}^2}{2\epsilon_0 V (|\mathbf{q}|^2 + |\mathbf{q}_D|^2)^2} \left(\frac{1}{\epsilon_+} - \frac{1}{\epsilon_-} \right), \quad (7)$$

where $D_i K$ is the deformation potential coupling constant, N_{op} is the equilibrium phonon population, ρ is the density of the material, $\mathbf{q}_D = 1/l_D$ is the screening wave vector for the electrons, and ϵ_- and ϵ_+ are the low- and high-frequency dielectric constants. All the phonon constants are reported in Table I. In our model, electrons are allowed to jump a maximum distance of five wells forward and five wells backward; nevertheless, we have verified that the results for the diffusion coefficient and the drift velocity are not affected by a further increase of the maximum hopping distance.

III. RESULTS

We have implemented a Monte Carlo³⁰ simulator for an ensemble of N independent, distinguishable particles (a typi-

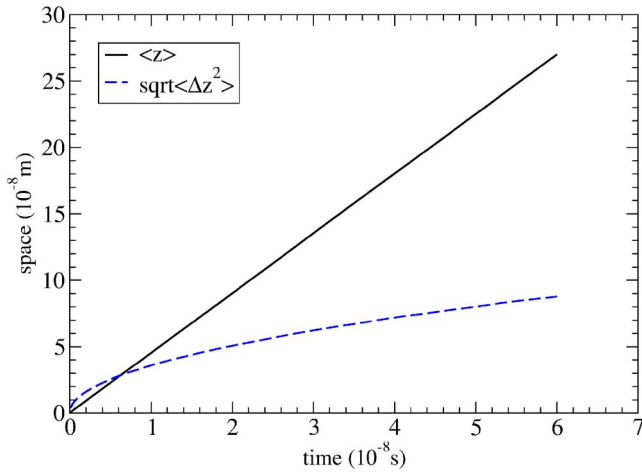


FIG. 1. (Color online) Output of the Monte Carlo program: the mean position $\langle z \rangle$ of the ensemble (continuous line) and its mean-square displacement $\sqrt{\langle \Delta z^2 \rangle}$ (dashed line) are represented for an electric field of 2000 kV/m.

cal simulation takes into account 2500 particles). The code simulates hopping transport in a SL, where particles jump from any initial state (ν, n, \mathbf{k}) to any final state (ν', n', \mathbf{k}') .³³ As demonstrated in Ref. 3, a simulation of transport in superlattices, based on the Wannier-Stark approach, is accurate at high electric fields, while at low fields it loses accuracy and a semiclassical Monte Carlo simulation is more suitable. In particular, the low field velocity curve providing the Ohmic mobility has been studied within a semiclassical framework in a previous work.²³

Here, we have considered an infinite SL where each carrier makes a significant high number of jumps between different states so that the time evolution of their average displacement can be recorded and used for the evaluation of the average drift velocity and the longitudinal diffusion coefficient as reported below. An example of output of the program is shown in Fig. 1, where the mean position and mean-square displacement of the ensemble, used for the calculation of drift velocity and diffusion coefficient, are plotted. Here, the linear and squared root dependence on time of $\langle z \rangle$ and $\sqrt{\langle \Delta z^2 \rangle}$, respectively, supports the evidence of the steady-state evolution of the carrier ensemble.

Accordingly, from its definition the instantaneous drift velocity in the finite difference formulation is calculated as

$$v_d(t) = \frac{L}{N\delta t} \sum_{i=1}^N \delta v_i(t), \quad (8)$$

where δt is the discretized time interval used in the simulation and $\delta v_i(t)$ is the distance jumped by the i th particle, in terms of number of wells. The drift velocity versus high electric field is reported in Fig. 2. At intermediate fields, we observe a remarkable smooth decrease of the drift velocity³⁸ and thus the presence of an NDM regime. Here NDM is interpreted as due to a localization effect driven by the electric field.² By further increasing the field, we find that the drift velocity passes through a minimum and then substan-

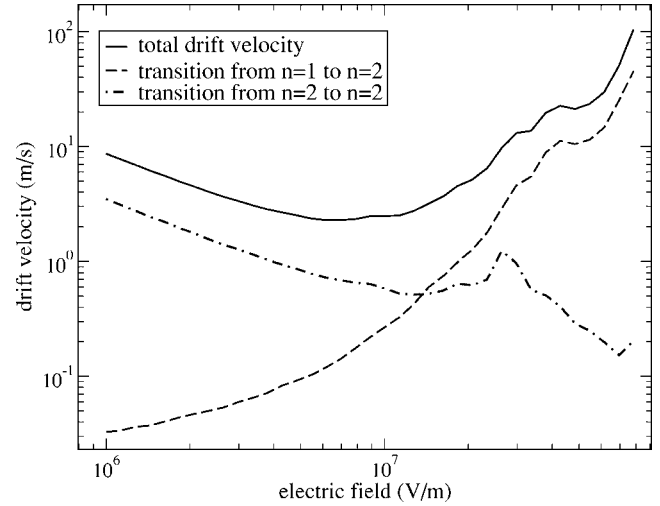


FIG. 2. Electron drift velocity of the superlattice at 300 K. Continuous, dashed, and dot-dashed curves refer, respectively, to total drift velocity, contribution due to intraband transitions associated with the level $n=2$, and contribution due to interband transitions associated with levels $n=1$ and $n=2$.

tially increases showing a structure with several dips and peaks which are resolved within the numerical uncertainty of the drift velocity. The presence of this structure is a signature of a quantum transport regime, as will be detailed below. In the same figure, the contributions to the drift velocity coming from different subbands are reported to explain the sudden increase in terms of two kinds of phenomena. The first is the presence of a resonance between the energy difference of two adjacent wells and the Si phonon energy $\hbar\omega_{\text{op}}$ (Ref. 4) (which is the most important scattering mechanism) that occurs when $eEL = \hbar\omega_{\text{op}}$. This resonance occurs when $E \approx 2.5 \times 10^7$ V/m, and is clearly evidenced in the velocity curve associated with intrasubband hopping. The second phenomenon is the presence of an intersubband hopping, which becomes significant only at very high electric fields, when $eEL = \Delta\epsilon_{12} - \hbar\omega_{\text{op}}$. This phenomenon is evidenced by the significant increase of the velocity curve associated with intersubband hopping and reported in Fig. 2. In principle, intraband resonances at higher harmonic frequencies $eEL = \hbar\omega_{\text{op}}/n$ should also be observable,⁴ but actually these resonances are as weak as the corresponding hopping distance. Moreover, the second resonance ($n=2$) occurs near 1.3×10^8 V/m, and it is hidden by the main resonance peak.

The (longitudinal) diffusion coefficient is obtained from the simulation, making use of its definition as a spatial spreading quantity,¹⁴

$$D_z = \frac{1}{2} \frac{\delta\langle(\Delta z)^2\rangle}{\delta t} \quad (9)$$

with $\Delta z = z - \langle z \rangle$ the instantaneous fluctuation of the carrier position along the field direction.

The diffusion coefficient obtained from the simulation is reported in Fig. 3, together with those calculated from the generalized Einstein relation and the simple WS-hopping model.⁸ The general behavior of the diffusion coefficient par-

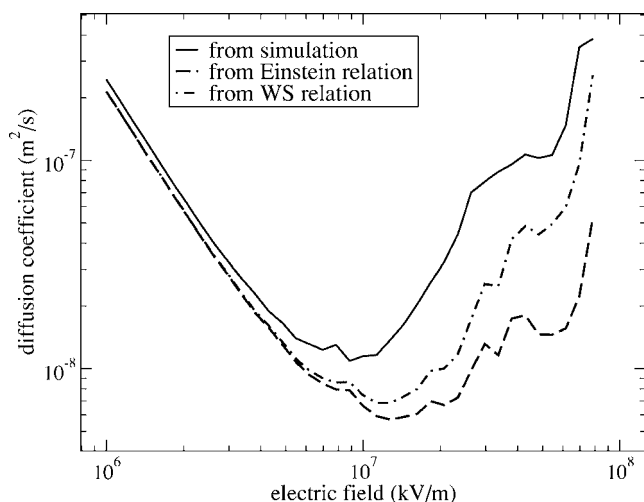


FIG. 3. Longitudinal diffusion coefficient of electrons in the superlattice at $T=300$ K. Different curves refer to results obtained by simulations and using different approaches. The continuous line refers to the spreading diffusion coefficient obtained directly from the simulation. The dashed curve refers to the diffusion coefficient obtained from the generalized Einstein relation with the mobility and mean energy calculated from the data of the simulations. The dash-dotted curve refers to the diffusion coefficient obtained from the WS-hopping expression (Ref. 8) with the mobility and mean energy calculated from the data of the simulations.

allels that of the drift velocity. We notice that the diffusion coefficient obtained from the generalized Einstein relation, where the mobility is calculated as v_d/E from the data of Fig. 2, reproduces the first part of the simulated curve corresponding to the NDC regime. By contrast, the second part of the simulated curve, that at the highest fields, turns out to be substantially underestimated. In an effort to overcome this drawback, we make use of an analytic expression calculated from a simple Wannier-Stark formulation of transport,⁸

$$D_z = \frac{v_z L}{2} \coth \frac{L}{L_E} = \frac{\mu k_B T}{e} \left(\frac{L}{L_E} \coth \frac{L}{L_E} \right), \quad (10)$$

where $L_E = 2k_B T/eE$ is the thermal field length.³⁴ In the limit $L/L_E \ll 1$, the above formula reproduces the Einstein relation and thus agrees with the simulations. However, at the highest fields, when $L/L_E \gg 1$, even if this formula gets closer than the generalized Einstein relation to the simulated values, the diffusion coefficient obtained by simulations remains underestimated by a factor of 3 to 4 (see Fig. 3). We believe that the main reasons for the remaining disagreement stem from the fact that Eq. (10) is calculated in the approximation of nearest-neighbor coupling between the wells of the SL, and that it does not account for the contribution to diffusion of the intersubband transitions. A relation similar to Eq. (10) was obtained²¹ when considering the effect of quantum phonon emission on the field-driven transport, for a bulk material. In that case, the characteristic length is the composite mean free path that arises from the mixing of diffusion mean free path and inelastic scattering length for quantum emission. Accordingly, two different diffusion regimes are identified: the first, at low fields, dominated by the diffusion and

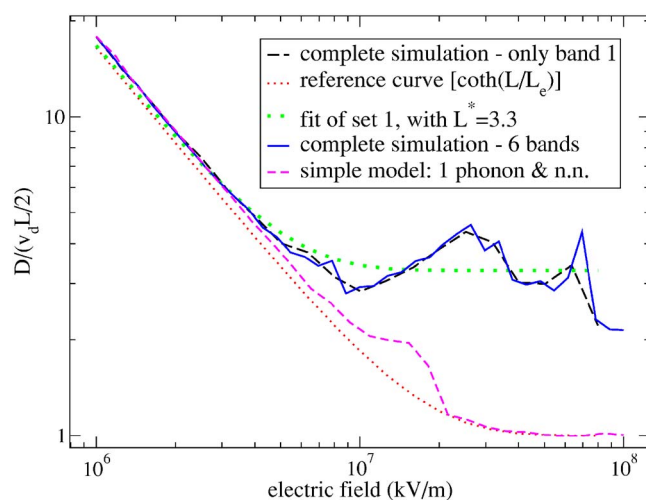


FIG. 4. (Color online) Comparative analysis for the normalized diffusion coefficient of a superlattice in the WS regime with models of increasing complexity. The dotted line gives the reference curve and is obtained from $\coth(L/L_e)$ of Ref. 8. The dashed curve (very close to the reference curve) refers to a simple model when the simulation is performed using a one-band, hop to nearest neighbor only, one optical phonon only. The long-dashed curve refers to a complete set of transitions but in the one-band model. The continuous curve refers to a complete set of transitions in the six-band model. Both last models are well approximated by the reference curve when the superlattice period L is replaced by an effective length $L^* = 3.3L$ (big-dot curve).

the second, at high fields, dominated by the phonon emission.

To better understand analogies and differences among the field dependence diffusion coefficients obtained by different approaches, we have performed a set of Monte Carlo simulations for the simple model⁸ and then for models with increasing degree of complexity up to that used for the drift velocity. The results are reported in Fig. 4 for the sake of a comparative analysis: here it is convenient to plot the dimensionless ratio $D/(v_z L/2)$. In this case, when plotting the law of Eq. (10) as a reference curve, we see that in the first part of the plot, where diffusion follows the Einstein behavior, the curve exhibits a $1/E$ decay in agreement with all the models considered here. By contrast, in the second part of the plot, there is a saturation behavior, where the smooth value of diffusion is limited by a size effect which, for the simple model, is controlled by the term $v_z L/2$. Here, the simple model (one band, one phonon, only nearest-neighbor hops) agrees well with the results of the simulations, except for fields near the resonance. For more complex systems, the diffusion coefficient of the simple model underestimates those of the simulations. These results suggest the possibility to introduce an effective length L^* that fits the smooth behavior of the diffusion and takes the meaning of a length representing the mean hopping distance of the electrons in their motion inside the SL. The value of this effective length depends upon all the geometrical and microscopic properties of the system and it enables us to fit the smooth behavior of the diffusion coefficient with a generalized law

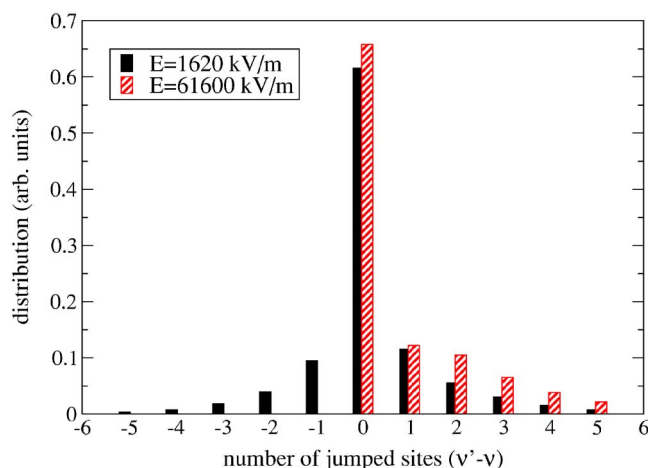


FIG. 5. (Color online) Distribution of the final site after the transition (the hopping distance $\nu' - \nu$) at two different electric fields. At low electric field the distribution is almost symmetric, while at high field the distribution is strongly asymmetric and backward transitions are almost completely forbidden (the transition to -1 is present but not appreciable in the figure).

$$D_z = \frac{v_z L^*}{2} \coth \frac{L^*}{L_E}, \quad (11)$$

where for the present case we found $L^* = 3.3L$. The resonance peak as well as the effects of interband transitions remain unexplained in this simple representation.

The discussion carried out above evidences that in a SL the diffusion takes two limiting regimes. The first corresponds to the field region characterized by NDM and the second corresponds to the highest fields, beyond the resonance peak, when the drift velocity starts increasing again with field. In the first region, we can identify a transport regime dominated by the continuous random-walk diffusion where the Einstein relation holds. In this case, $(L^*/L_E) \rightarrow 0$ and $D_z \approx \frac{1}{2} v_z L_E$, meaning that diffusion is governed by the field dependence of both the drift velocity and the carrier thermal field length. In the second region, the thermal field length is replaced by an effective hopping length L^* which cannot become smaller than the period of the SL and the diffusion coefficient is $D_z \approx \frac{1}{2} v_z L^*$.

In other words, when the electric field is low, electrons can move forward and backward with almost equal probability, so they can diffuse in both directions. When the electric field is sufficiently high, backward transitions are strongly suppressed as illustrated in Fig. 5. Here we see that at high fields only forward jumps remain active, and at both fields jumps occur up to the fifth site. At high fields we notice that, in the simple model, electrons can only jump one step forward, and the SL parameter L becomes the dominant scale length. In the complete model (see Fig. 5), electrons can jump more steps forward and the relevant scale length becomes $L^* > L$.

This point of view can also be applied in the case of Ref. 21.

The reason why the Einstein relation describes well the diffusion in the NDC region can be understood by considering the noise temperature defined as

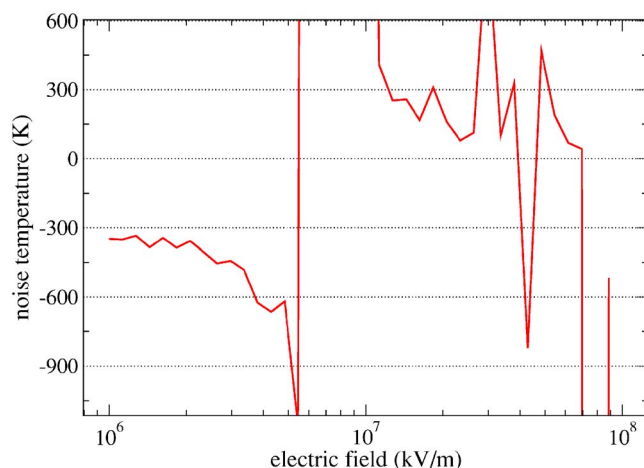


FIG. 6. (Color online) Noise temperature calculated for the superlattice. In the first region, the curve is very close to -300 K, indicating a kind of anti-Ohmic region.

$$T_n = \frac{eD}{\mu' k_B}, \quad (12)$$

with μ' the differential mobility. The results evaluated from the simulations are reported in Fig. 6. It turns out that in the NDM region, $T_n \approx -300$ K. In other words, it means that here the transport follows a kind of “anti-Ohmic” behavior in the sense that at increasing fields the drift velocity decreases as $1/E$. The negative value of the noise temperature signifies that the system is electrically unstable, but the carrier mean energy remains that of the thermal equilibrium value (no hot-carrier effects).³⁹ This behavior ends near the crossing point $L^* = L_E$ where a resonance occurs and the noise temperature exhibits a singularity. At fields above the resonance, the presence of dips and peaks in the drift velocity and diffusion coefficient implies strong fluctuations of the noise temperature which are a signature of quantum transport effects.

Finally, we want to point out that the crossover between the two diffusion regimes occurs at a field for which $L^* = L_E$, and that, in correspondence of this crossover, the mean energy of the carriers is found to start increasing with the electric field. The increase in mean energy corresponds to a deviation of the distribution function, from its exponential thermal slope as reported in Fig. 7. Here, the significant deviations from the thermal behavior (dashed curve) should be associated with the interplay of the different transition mechanisms involved in the hopping transport.

IV. CONCLUSIONS

The high-field behavior of the drift velocity and diffusion coefficient in a SL have been investigated within a Wannier-Stark approach. To this purpose, an ensemble Monte Carlo simulator has been implemented. The drift velocity is found to exhibit a NDM behavior followed by a minimum and a smooth increase coupled with dips and peaks associated with quantum transport effects such as resonance between adjacent wells and intersubband transitions. The longitudinal dif-

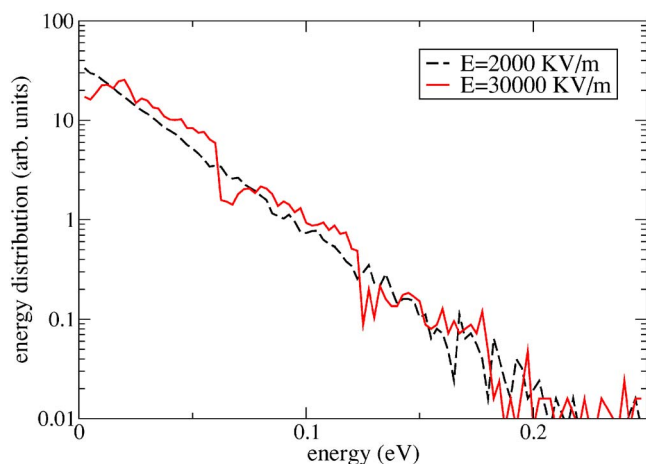


FIG. 7. (Color online) Energy distribution function of electrons obtained for a single-band simulation at the two electric fields reported in the figure.

fusion coefficient is found to exhibit a two-regime behavior. In the NDC region, the diffusion is well described by a generalized Einstein relation which accounts for a field-dependent mobility and diffusivity. In the highest field region, where the drift velocity and the diffusion coefficient start increasing again with the electric field, the results of the simulations are only qualitatively described by an existing WS-hopping model, which is found to represent a too simple model for the system considered here. Remarkably, the superlattice period L is found to represent an intrinsic size parameter for the structure which dominates the behavior of

diffusion at high fields. This parameter is replaced, in the case of a more realistic model (coupling beyond nearest neighbor and many bands) by an effective parameter $L^* \geq L$ that can be interpreted as a “mean hopping distance.” In particular, the crossover between the Einstein and the hopping description of diffusion is determined by the condition $L^* = L_E$. In the NDM region of low electric fields, the very good agreement between the Einstein relation and the results of the simulation is confirmed by the value of the effective noise temperature, whose negative room-temperature value makes it sensible to refer to the NDM region as an “anti-Ohmic” region. In this region, the application of a semiclassical approach to transport is justified. We want to stress that, in contrast with bulk materials, in SL we predict the possibility of an increase of both drift and diffusion at the highest fields because of the increased efficiency of hopping to further sites. In any case, the values of both drift and diffusion in SLs remain significantly smaller (for about three orders of magnitude) than those of bulk materials.

An experimental validation of the results presented here can profit from the noise conductivity method²⁰ (at frequencies high enough to get rid of $1/f$ excess noise) and/or of the four-wave mixing method as detailed in Refs. 11 and 12.

ACKNOWLEDGMENTS

Support by the Italian Ministry of Education, University and Research (MIUR) under the project “Noise models and measurements in nanostructures” is gratefully acknowledged.

*Electronic address: marcello.rosini@unile.it

¹H. T. Grahn, K. von Klitzing, K. Ploog, and G. H. Döhler, Phys. Rev. B **43**, 12094 (1991).

²L. Esaki and R. Tsu, IBM J. Res. Dev. **14**, 61 (1970).

³A. Wacker and A.-P. Jauho, Phys. Rev. Lett. **80**, 369 (1998).

⁴S. Rott, P. Binder, N. Linder, and G. H. Döhler, Physica E (Amsterdam) **2**, 511 (1998).

⁵A. Wacker, Phys. Rep. **357**, 1 (2002).

⁶L. G. Mouroukh, A. Y. Smirnov, and N. J. M. Horing, Phys. Lett. A **269**, 175 (2000).

⁷S. Choudhury, L. J. Singh, and K. P. Ghatak, Nanotechnology **15**, 180 (2004).

⁸V. V. Bryksin and P. Kleinert, J. Phys.: Condens. Matter **15**, 1415 (2003).

⁹P. Kleinert and V. V. Bryksin, J. Phys.: Condens. Matter **16**, 4441 (2004).

¹⁰L. L. Bonilla and R. Escobedo, Phys. Rev. B **68**, 241304(R) (2003).

¹¹D. X. Zhu, S. Dubovitsky, W. H. Steier, J. Burger, D. Tishinin, K. Uppal, and P. D. Dapkus, Appl. Phys. Lett. **71**, 647 (1997).

¹²A. R. Cameron, P. Riblet, and A. Miller, Phys. Rev. Lett. **76**, 4793 (1996).

¹³S. M. Sze, *Physics of Semiconductor Devices* (Wiley, New York, 1981).

¹⁴L. Reggiani, *Hot-Electron Transport in Semiconductors* (Springer, Berlin, 1985).

¹⁵P. J. Price, in *Fluctuation Phenomena in Solids*, edited by R. E. Burgess (Academic, New York, 1965), p. 355.

¹⁶J.-P. Nougier, IEEE Trans. Electron Devices **41**, 2034 (1994).

¹⁷V. Bareikis, J. Liberis, I. Matulioniene, A. Matulionis, and P. Sakalas, IEEE Trans. Electron Devices **41**, 2050 (1994).

¹⁸M. de Murcia, D. Gasquet, A. Elamri, J.-P. Nougier, and J. Vanbremeersch, IEEE Trans. Electron Devices **38**, 2531 (1991).

¹⁹C. F. Whiteside, G. Bosman, H. Morkoc, and W. Kopp, IEEE Electron Device Lett. **EDL-7**, 294 (1986).

²⁰H. L. Hartnagel, R. Katilius, and A. Matulionis, *Microwave Noise in Semiconductor Devices* (Wiley, New York, 2001).

²¹V. K. Arora, Microelectron. J. **31**, 853 (2000).

²²A. Sharma and V. K. Arora, J. Appl. Phys. **97**, 093704 (2005).

²³M. Rosini, C. Jacoboni, and S. Ossicini, Phys. Rev. B **66**, 155332 (2002).

²⁴G. H. Wannier, Phys. Rev. **117**, 432 (1960).

²⁵E. O. Kane, J. Phys. Chem. Solids **12**, 181 (1959).

²⁶A. Dargys and J. Kundrotas, *Handbook of Physical Properties of Ge, Si, GaAs* (Science and Encyclopedia Publishers, Vilnius, 1994).

²⁷M. Hirose, Mater. Sci. Eng., B **41**, 35 (1996).

²⁸B. Brar, G. D. Wilk, and A. C. Seabaugh, Appl. Phys. Lett. **69**,

- 2728 (1996).
- ²⁹J. B. Xia and K. W. Cheah, Phys. Rev. B **56**, 14925 (1997).
- ³⁰C. Jacoboni and L. Reggiani, Rev. Mod. Phys. **55**, 645 (1983).
- ³¹M. V. Fischetti and D. J. D. Maria, Solid-State Electron. **31**, 629 (1988).
- ³²H. Rucker, E. Molinari, and P. Lugli, Phys. Rev. B **45**, 6747 (1992).
- ³³M. Rosini, Ph.D. thesis, Università di Modena e Reggio Emilia, Modena, Italy, 2004.
- ³⁴G. Gomila and L. Reggiani, Phys. Rev. B **62**, 8068 (2000).
- ³⁵G. Bastard, *Wave Mechanics Applied to Semiconductors Heterostructures* (Les Editions de Physique, Paris, 1990).
- ³⁶P. Shiktorov, V. Gružinskis, E. Starikov, L. Reggiani, and L. Varani, Phys. Rev. B **54**, 8821 (1996).
- ³⁷A general reading on these topics can be found in Ref. 35.
- ³⁸The positive differential mobility at low field is observable in the SL,¹ but we are interested in the high field behavior.
- ³⁹See, for example, Ref. 36.